USING FINITE ELEMENT ANALYSIS AND STRAIN GAUGE EXPERIMENTAL DATA TO EVALUATE STRESS CONCENTRATION FACTOR ON PRESS-FIT ASSEMBLY

Cajuhi, Aguinaldo Jose, ajcajuhi@bol.com.br
Pepe, Iuri Muniz, mpepe@ufba.br
Laboratório de Propriedades Óticas, Instituto de Fisica, Universidade Federal da Bahia – UFBA, PPGM, Escola Politécnica, Universidade Federal da Bahia – UFBA

Moreno, Denis Mestre , dmoreno8@ford.com
Ford Motor Company Brasil Ltda – Camaçari - Bahia

Abstract. *The behavior of any physical structure is usually non linear. However, the response of a given structure can often be approximated to a linear case if its deformations or local displacements are small. This simplification is even more acceptable when the assembled parts are able to interfere each other, a good example of interference fit is a shaft assembled inside its housing. Interference fit tools can be used to better understanding of joint parts mounted in circular geometry. Analytically is possible to have an initial approach in determining the amount of efforts applied to a giving joint system. Almost all machine components and structural members suffer some form of geometrical recoil due to backlashes and production tolerances, or, in some cases, one can experience abrupt change in cross section or internal micro structural discontinuities. Those factors, associated with the local stress are coming from Press-fit process causing pre-tension on internal and external surfaces. The maximum local stress normally occurs at these discontinuities and local defects. The nominal stress can be calculated, for a particular loading and net cross section, assuming a stress distribution for a uniform geometry. This paper presents the analytical treatment of the stress concentration factor, based on the elasticity theory, in association with finite element analysis and the experimental data from a strain gauge. That system was able to measure small deformation from assembled parts and its correlations.*

Keywords: strain gauge; small deformation; press-fit; correlation

1. INTRODUCTION

An essential element of successful fatigue analysis is the accurate determination of stress concentrations around stress raising features. Quick and easy access to such data is important when different alternative geometry could be considered. Present methods for determining stress concentrations around stress raising features mainly depend on graphical charts and analytical information presented in the literature. In addition, finite element analysis (FEA) is widely used for cases where a standard solution cannot be found in the fore mentioned texts.

These methods can be time consuming and error prone, when data may need to be interpolated and extrapolated from graphical representations. Finite element analysis critically depends on the development of an accurate problem modeling, what undoubtedly takes time and consumes limited development resources. Therefore, there is a requirement of systems able on providing relevant information from powerful analysis tooling. Those analysis tools must be capable of easy and quick results interpretation, what would be extremely useful during the early stages of the product design process, especially when alternative geometries are being considered.

Analytical modeling and graphical methods are helpful in focusing resources on priority areas, and could be applied before starting with more intensive resource and time consuming techniques, such as finite element analysis.

In some structural issues it is adequate to consider uniform sections and take the average stress across that section. However, in the aerospace industry, were fatigue failure is a major consideration, it is important to consider the local stress around shoulders, holes and grooves where the stress distribution and the localized stress concentrations are introduced. If the stress concentration is significant, then premature failure of components may occur. The stress concentration factor Kt, is defined as the ratio of the peak stress and the general stress for a given component.

2. PRESS-FIT CONCEPTS

An "interference fit" is created when two cylindrical parts are assembled by shrink-fitting or press-fitting of one part upon another (a common means of coupling a hub to a shaft). A Press-fit is obtained by machining the hole in the hub (the outer member) with a slightly smaller diameter respect to the shaft (the inner member, note that the shaft does not have to be solid). The two parts are then forced together slowly using a press (normally with oil applied at the intersection to act as a lubricant). The subsequent elastic deformation of both the shaft and the hub acts creating large

normal and frictional forces between the parts. The frictional force transmits the shaft torque to the hub and also resists to axial motion. The "Figures 1, 2, 3 and 4" show the most common of interference fit.
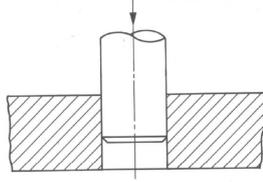
Figure 1. Longitudinal interference assembly
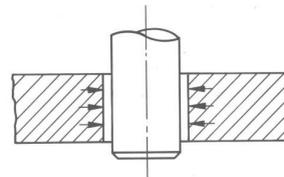
Figure 2. Longitudinal interference by expansion
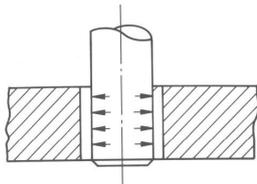
Figure 3. Transversal interference by contraction
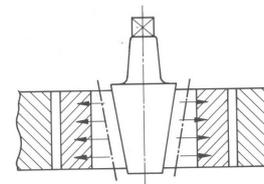
Figure 4. Transversal interference by plasticity interior part

3. COMPUTER AIDED ENGINEERING (CAE) TOOL FOR STRESS ANALYSIS

Computer Aided Engineering (CAE) technology is supported by many commercial software packages that successfully implement different simulation methods, the Finite Element Method (FEM) that is widely used in structural design is a good example of this technology. System responses like stress, displacements, rotations, natural frequencies, strain energy, mass, volume, etc, should be optimized and/or used as constraints.

Theses responses are generally restricted by one or more "admissible" engineering parameters such as: rupture or yield stress, fatigue limit, resonance frequency, maximum displacements at some locations, admissible weight, cost, etc.

When the parts are assembled using press-fit process a tube or a shaft is introduced inside of a hub by sliding. Considering the tolerances between tube and hub, associate to the pressing fit process, then a superficial finishing occur between these two surfaces, by the breaking of material superficial peaks associated to its roughness. Depending on the tolerances adjustments, the parts will be hold together. The elastic stress due to parts processing must be considered on further calculation.

This work presents a method to determine the Stress Concentration Factor – Kt from CAE results, applied in the development of mechanical components, based on structural durability, using computer simulation resources and finite element modeling techniques as well.

3.1. Strategy to perform CAE analysis

Six sigma methods have been designed to identify the most influent factors on stress study and define the best CAE supporting experiments to test the previews hypothesis.

A finite element result, based on nonlinear behavior, was used to determine stress in a tube inserted by press-fit in a hub. This press-fit element has been tested and numerically simulated by the application of bending forces and a von Mises criterion is used to predict yield stress. A range of friction coefficients between the fitted parts were assumed.

Experimental test and CAE press-fit analysis are used to validate analytical results. The model was calibrated using data from friction coefficients, material type, geometry, etc.

3.2. Stress Concentration Factor analysis cascade

In CAE analysis important and relevant factors can be introduced to simulate press-fit, as: material specification: elastic modulus for inner and outer members, as well as the Poisson's ratio for both members and tensile stress.

The geometric parameters taken into account are: geometric tolerances, radial interference, outer radius for outer member, inner radius for inner member, thickness, nominal radius at the interference and tolerance grade.

The assembly conditions are: sequence of adjustment, no alignment between tube and hub, longitudinal force to assemble the tube inside the hub and friction coefficient.

3.3. Problem description

The cascade proposed on item 3.2 was used to identify the input terms of the CAE model, trying to obtain analytical results and compare to experimental test. Abaqus (Simulia Software) pre, post-processing and solver were used for non-linear analysis to obtain best results using geometric interference.

3.4. Concept – CAE Analysis

The parameters from initial study were identified and applied, as inputs, to the model are:

Geometry: tube and hub -> thickness varying from 8.30 and 4.16 mm;
Materials: Tube – SAE 1020 / SAE 1035M; Hub – Cast Iron;
Loads: Interference between wall thickness varying from 0.300 and 0.150 mm;
Concentrated load at outside tube = 8541 N;
Load Steps: Step1: Shrinkage and expansion to simulate the press up; Step2: Applying load to simulate bending + press up results;
Boundary Conditions: pinned (displacements = 0 and free rotation on x, y and z directions) on the hub and free at tube extreme

3.5. CAE model details

Basically one non-linearity type was identified in this model, the radial interference between tube and hub as can be seen in "Fig. 5".
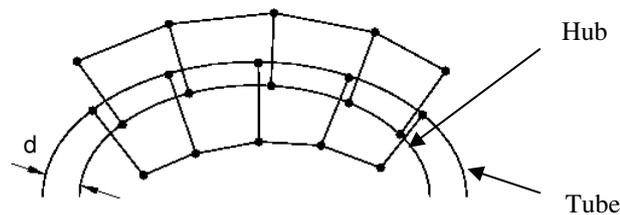
Figure 5. d = radial interference

Two steps are used on Abaqus software to determine stresses on press-fit structure.

```
** STEP - 1
** PERFORM INTERFERENCE FIT BETWEEN TUBE AND HUB
*CONTACT INTERFERENCE, SHRINK
SLAVE, MASTER

** STEP - 2
** LOAD APPLICATION = 8541 N IN Z DIRECTION
*CLOAD, OP=NEW
NODE, DIRECTION, LOAD VALUE
```

3.6. CAE Model

The "Figure 6" shows a viewgraph indicating the boundary conditions.
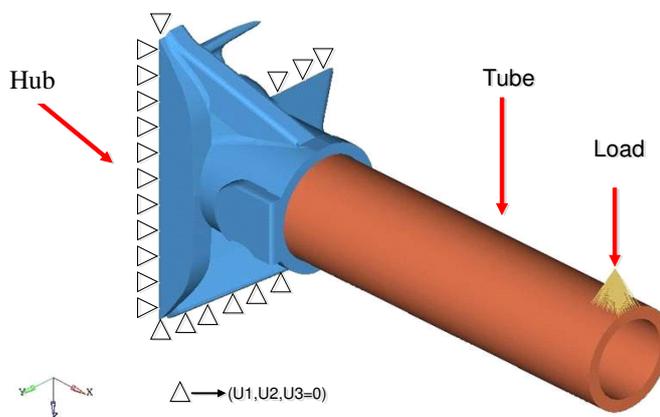
Figure 6. Model and boundary conditions

3.7. CAE Model – Elements/Nodes Results

The "Figure 7" indicates the position of the local stresses used on this analysis.
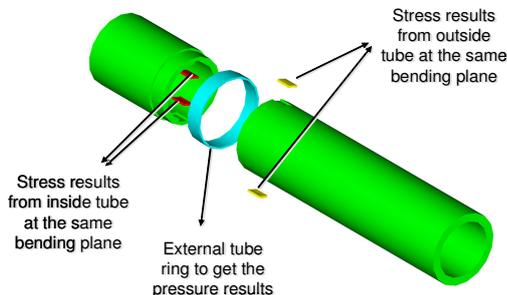
Figure 7. Places for local stresses

3.8. Kt Definition

The Kt is the relation between the Maximum Local Stress and the Nominal Stress is presented on equation 1 (σmax = CAE Max Stress and σnom = Theoretical Stress), "Peterson. (1997)".

$$kt = \frac{\sigma \max}{\sigma nom}$$ (1)

3.8.1. σmax from CAE Max Stress

The state of stress in a plane is considered using experimental data of a strain gauges sensing system. The problem is modeled by an ensemble of tetrahedron and heptahedron finite elements. All displacements on the tube positioning are hold by nodes on the hub (see figure 7) and a concentrated force is applied at the extreme of the piece.

3.8.2. σmax from Theoretical Stress

The "Figure 8" indicates the nominal stress generating by the bending moment.
Based on the figure 8, the equations below show the calculation on the tube section, "Young, W.C., Roark (2001)".

$$\sigma_{sec\,tion} = \frac{M}{\left(\dfrac{Inertia}{Y}\right)}$$ (2)

$$\sigma_{sec\,tion} = \frac{Load \times l}{\dfrac{\pi}{32}\left(\dfrac{TubeOD^\wedge4 - TubeID^\wedge4}{TubeOD}\right)}$$ (3)
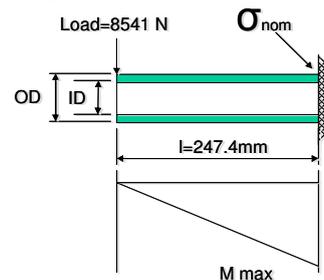
Figure8. σnom

3.9. Design of Experiments - DOE

The proposal of this DOE is determine the Kt of a pressing-fit piece, from the material characteristics and tolerance specifications – Simulating the Manufacturing Variability. "Table 1" indicates the sequence of experiments considering all possible CAE analyses combinations. Value -1 indicates minimum parameter value and +1 maximum parameter value.

Table 1. CAE analyses combinations

		RunOrder	CenterPt	Blocks	Material	Tolerance	Thickness
1		1	1	1	-1	-1	-1
2		2	1	1	1	-1	-1
3		3	1	1	-1	1	-1
4		4	1	1	1	1	-1
5		5	1	1	-1	-1	1
6		6	1	1	1	-1	1
7		7	1	1	-1	1	1
8		8	1	1	1	1	1

Factors that were used in this DOE:

Material -> +1= SAE 1035M and -1 = SAE 1020
Interference -> +1 = 0.300 mm and -1 = 0.150 mm
Wall Thickness -> +1 = 8.35 mm and -1 = 4.16 mm

3.9.1. CAE stress place results

The results using factors from CAE analyses combinations are showed in "Figures 9, 10, 11 and 12". Von Mises criteria were used to show the maximum values on whole section (ws - considering hub and tube together) and tube section (ts). The stress values were filtered (gray color legend) to show the stress on interface between tube and hub.
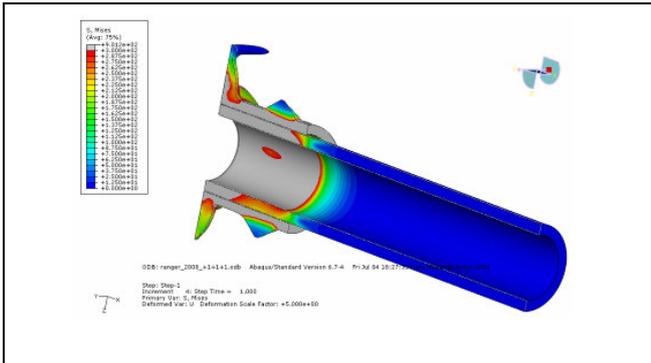
Figure 9. Press-fit CAE results on ws	Figure 10. Press-fit CAE results on ts
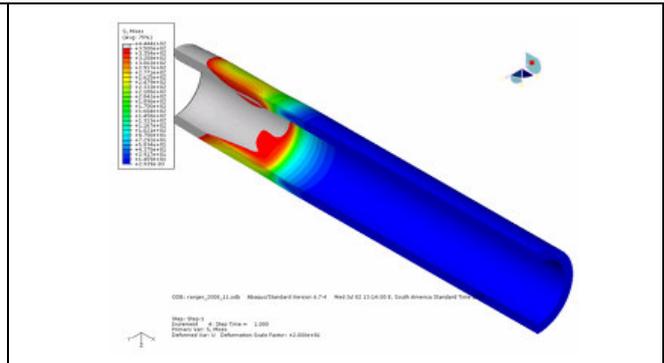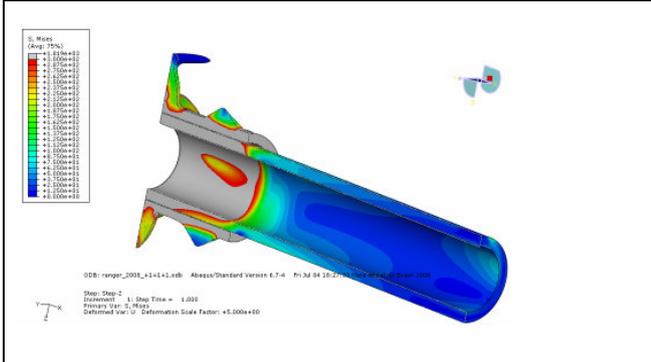
Figure 11. Press-fit + Bending CAE results on ws	Figure 12. Press-fit + Bending CAE results on ts
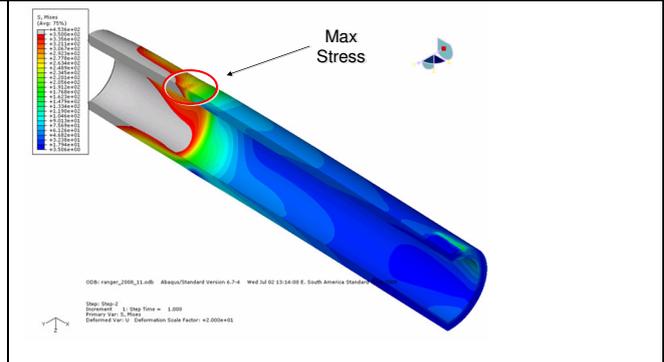
Axial stress results from CAE model were used to define the local axial tension. It is compatible with theoretical stress calculations. "Figures 13 and 14" show stress values on the whole section (ws - considering hub and tube together) and tube (wt). Axial stress is represented as S11 results; it can be seen at Abaqus pre-processing (Simulia Software).
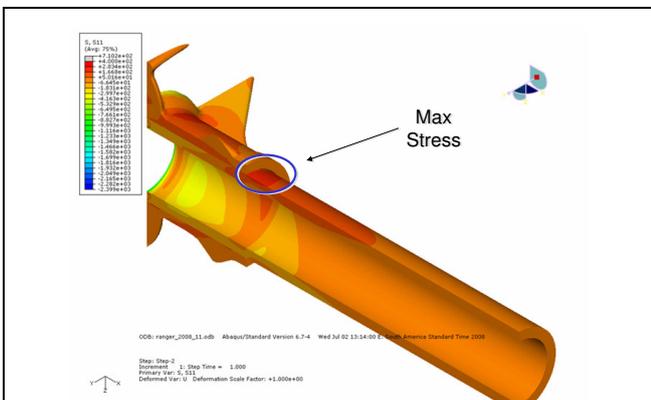
Figure 13. Press-fit + Bending CAE results on ws – S11	Figure 14. Press-fit + Bending CAE results on wt – S11
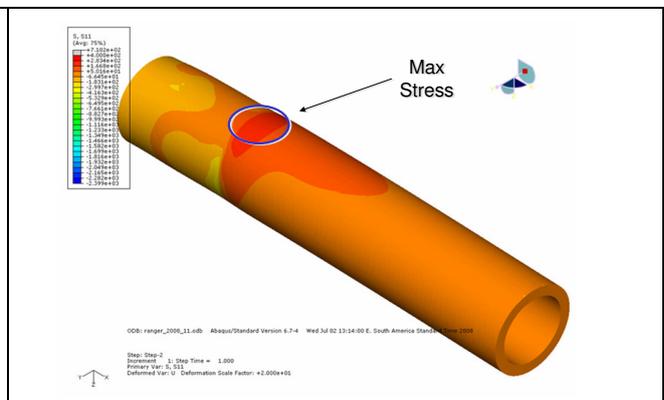
3.9.2. Design of Experiments – CAE Results

From equation 1 the stress concentration factors – Kt are showed on "Tab. 2". These simple calculations are done dividing maximum stress from CAE results by nominal stress from analytical calculation.
.

Table 2. DOE CAE results

I I	Material	Tolerance	Thickness	Max Stress	Nomimal Stress	Kt
1	-1	-1	-1	213.9	162.0	**1.32**
2	1	-1	-1	218.7	162.0	**1.35**
3	-1	1	-1	289.9	162.0	**1.79**
4	1	1	-1	276.5	162.0	**1.71**
5	-1	-1	1	154.2	97.5	**1.58**
6	1	-1	1	156.0	97.5	**1.60**
7	-1	1	1	224.6	97.5	**2.30**
8	1	1	1	216.0	97.5	**2.22**

3.9.3. Pareto Chart of the Effects

"Figures 15 and 16" indicate most important factors for the DOE analysis (Minitab statistical software)
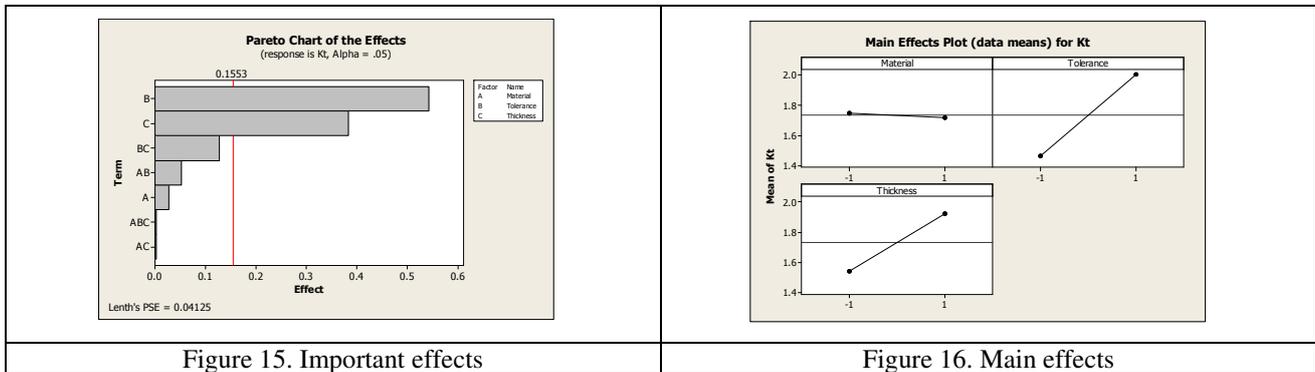
Figure 15. Important effects	Figure 16. Main effects

The parameters B and C, respectively tolerance and thickness are the most important factors on press-fit assembling.
From table 2 the minimum Kt value (Kt=1.32) was calculated when tolerance and thickness are minimum and (Kt=2.30) for tolerance and thickness as maximum. In all cases materials do not have any influence.

4. TEST VALIDATION SETUP

"Figure 17" shows the validation test using a real model to measure stresses with strain gauges rosettes on a tube and compare that to the CAE results. On that case a tube has been mounted by press-fitting to a car hub device, this device is accommodated and locked-up on a metal block to the floor. A second block fixes the tube to the floor as well. The assembling was instrumented with strain-gauges rosettes to measure the tube deformation.
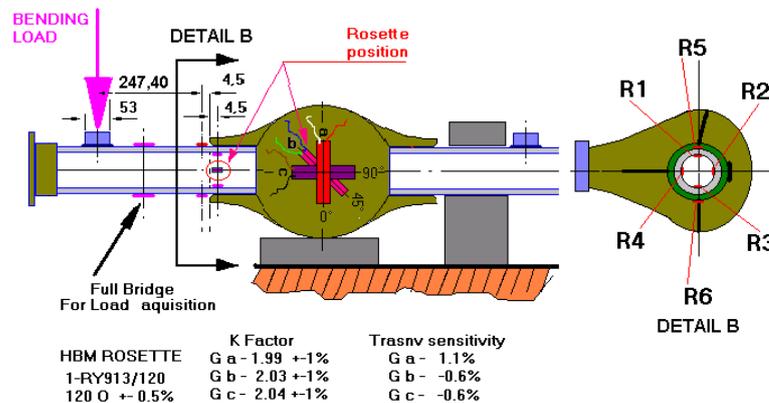
Figure 17. Rosettes and load places

Rosettes R5 and R6 were mounted on the tube external wall close to the hub. Rosettes R1, R2, R3 and R4 were mounted on the inside of the tube as close as possible to the final hub too.

"Figure 18" shows a photograph of the devices used to measure strain with rosettes.

"Figuer 19" shows the rosette gluing on the outside of the tube.
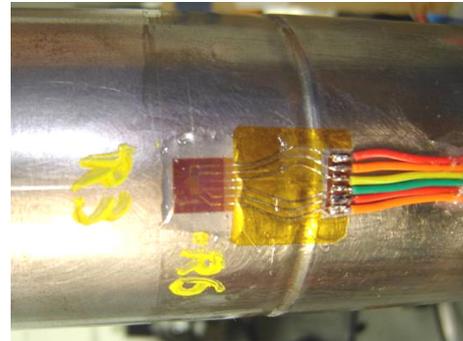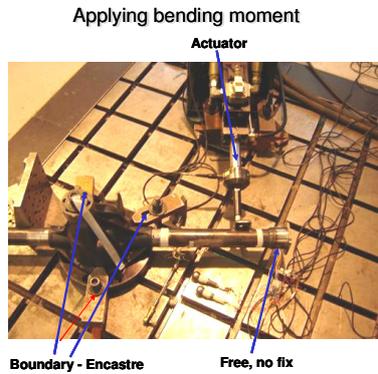
Figure 18. Devices and rosettes installed

Figure 19. 2 Rosettes: 00, 450 and 900

"Figure 20" shows the rosettes glued to the inside of the testing tube.

Figure 20. 4 Rosettes: 00, 450 and 900

5. TEST VALIDATION RESULTS

"Table 3" indicates the rosettes strain measurements using strain gauges R1 to 6; the load was increased intentionally to verify the strain linearity.

Table 3. Experimental results

SG	Rosette	Press-fit Max.	Bending 2847 N	Bending 5694 N	Bending 8541 N
		(µm/m)	(µm/m)	(µm/m)	(µm/m)
A	R1(Inside)	-643	-40	-85	-136
	R2(Inside)	-841	3	10	26
	R3(Inside)	-155	24	70	130
	R4(Inside)	-401	13	14	14
	R5(outside)	-406	11	11	5
	R6(outside)	-101	30	58	85
B	R1(Inside)	28	4	14	23
	R2(Inside)	384	-18	-27	-41
	R3(Inside)	-239	-44	-100	-148
	R4(Inside)	132	20	32	32
	R5(outside)	95	65	113	159
	R6(outside)	100	-78	-163	-250
C	R1(Inside)	1081	76	165	263
	R2(Inside)	1050	-15	-23	-37
	R3(Inside)	-189	-98	-221	-344
	R4(Inside)	433	-83	-42	-15
	R5(outside)	476	210	391	578
	R6(outside)	353	-187	-371	-565

5.1 Test validation analysis

"Table 4" indicates the stress calculations using the strain measured by the rosettes, the highlight values on that table were compared to those on "Tab. 5".

Table 4. Experimental analysis

Rosette	Press-fit	Bending	Press-fit + Bending	Press-fit	Press-fit [MPa]	Bending	Bending [MPa]	Press-fit + Bending	Press-fit + Bend [MPa]	ε_1	ε_2	σ_1	σ_2	Mises [MPa]	
R1	1081	263	1344	1.08E-03	**223.77**	2.63E-04	**54.44**	1.34E-03	**278.21**	1.37E-03	-8.04E-04	256.54	-89.46	**311.07**	Press-fit + Bending
R2	1050	-37	1013	1.05E-03	217.35	-3.70E-05	-7.66	1.01E-03	209.69	1.05E-03	-8.47E-04	179.91	-121.36	262.54	
R3	-189	-344	-533	-1.89E-03	**-39.12**	-3.44E-04	**-71.21**	-5.33E-04	**-110.33**	-2.99E-06	-5.55E-04	-38.56	-126.45	**112.26**	
R4	433	-15	418	4.33E-04	89.63	-1.50E-05	-3.11	4.18E-04	86.53	4.45E-04	-4.14E-04	72.90	-63.73	118.41	
R5	476	578	1054	4.76E-04	**98.53**	5.78E-04	**119.65**	1.05E-03	**218.18**	1.06E-03	-4.05E-04	212.96	-19.86	**223.56**	
R6	353	-565	-212	3.53E-04	**73.07**	-5.65E-04	**-116.96**	-2.12E-04	**-43.88**	-9.60E-06	-2.18E-04	-17.09	-50.34	**44.33**	

5.2. Test validation for stress analysis

"Table 5" indicates the comparisons between CAE stress and rosettes strains measurements.

Table 5. Comparisons – CAE / Rosettes

	Von Mises CAE	Von Mises Rosette	Von Mises Diff	Stress11 CAE	Stress11 Rosette	Stress11 Diff
Rosette R1	398.87	311.07	28.2%	95.22	278.21	65.8%
Rosette R3	310.28	112.26	176.4%	-2.27	-110.33	97.9%
Rosette R5	244.73	223.56	9.5%	193.73	218.18	11.2%
Rosette R6	75.91	44.33	71.2%	-40.28	-43.88	8.2%

Measurement with rosettes R1 and R3 are not consistent to the CAE model. The relative differences between these results (on percentage) are very high when compared to stress S11.

Rosettes R5 and R6 are consistent with CAE model, showing a small relative difference on stress S11, in percentage.

Rosettes R1, R2, R3 and R4 were very difficult to be installed. They were placed inside the tube. Some problems happened when these rosettes were assembled.

Making one overall analysis of the results, one can see that the failure by fatigue occurs at external tube surface. This occurs due to the normal traction stress on the surface, caused by stress S11.

5.3. Test validation analysis for contact pressure

Regardless the fitting method, an interference fit creates a contact pressure p (also named radial pressure, interference pressure, etc.) between the two parts at the transition radius r (also called the common radius). This contact pressure causes a radial stresses equal to -p in each member at the contacting surfaces. An interference fit creates the same stress state in the shaft, due to the uniform external pressure acting on its outer surface. The hub experiences the same stresses as in the thick-walled cylinder submitted to an internal pressure. The "Figure 21" shows the parameters used on press-fit equation.
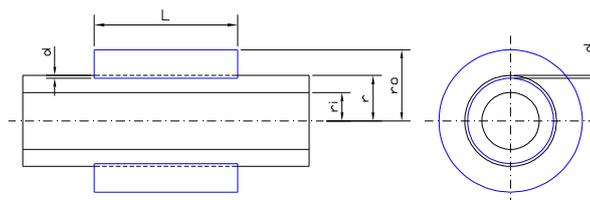
Figure 21. Input parameters

The equations 4, 5 and 6 are based on the deformation of the two members caused by the interference. In the case of a hub, that has been press-fitted to a tube, this assumption is seldom true as the tube is generally longer than the hub. This would produce an increasing of pressure at each ends of the hub. This condition generates a stress concentration

factor on the tube that must be investigated, whom is the main objective of this work. The value of the stress concentration factor depends upon on the contact pressure and the design of the hub, "Shigley *et al.* (1989)".

5.3.1. Interference Pressure

p = Contact pressure

$$p = \frac{d}{\frac{r}{E2}\left(\frac{ro^2 + r^2}{ro^2 - r^2} + n2\right) + \frac{r}{E1}\left(\frac{r^2 + ri^2}{r^2 - ri^2} - n1\right)} \tag{4}$$

di = Change of the outer radius of the inner member

$$di = \frac{-p \times r}{E1}\left(\frac{r^2 + ri^2}{r^2 - ri^2} - n1\right) \tag{5}$$

do = Change of the inner radius of the outer member

$$di = \frac{p \times r}{E2}\left(\frac{ro^2 + r^2}{ro^2 - r^2} + n2\right) \tag{6}$$

The "Table 6" indicates the ring pressure on the external tube calculation using "Equations (4, 5 and 6)".

Table 6. Interference pressure results calculations

Entries	E1 = Elastic Modulus for the inner member	2.10E+05 MPa
	E2 = Elastic Modulus for the outer member	1.70E+05 MPa
	n1 = Poisson's Ratio for the inner member	0.30 mm
	n2 = Poisson's Ratio for the outer member	0.30 mm
	m = Coefficient of friction - 0.12-0.15 for hydraulically expanded hubs and 0.15-0.20 for shrink or press fit hubs	0.25
	d = Radial Interference	0.30 mm
	L = Contact length	105.00 mm
	r = Nominal radius at the interference	35.00 mm
	r_o = Outer radius of the outer member	42.00 mm
	r_i = Inner radius of the inner member - ri = 0 for a solid member	26.70 mm
Answers	p = Contact pressure, Interference Pressure	168.15 MPa
	d = Radial Interference	
	d_i = Change of the outer radius of the inner member	-0.0976 mm
	d_o = Change of the inner radius of the outer member	0.2024 mm

5.3.2. External tube ring pressure results from CAE results

"Fig. 21" shows annular pressure results at external ring tube.
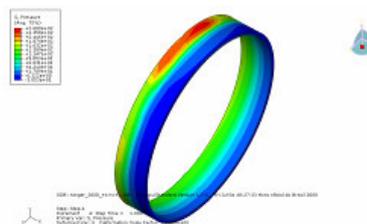
Figure 21. Annular pressure results

Comparing CAE calculation for the average contact pressure for an external ring of the tube (157.38 MPa) and the analytical calculation done above (168.15 MPa) (presented on "Tab. 6") the difference is less than 10% (6.40 %).

This value is acceptable and can be associated to the calculation uncertainty.

6. DISCUSSION

The Kt calculation is a way to start the stress analysis using CAE. But the most important thing is define correctly the terms and how influences it on the final results.

It is well known that it is impossible to have a complete set of relevant terms as input of the CAE analysis. Of course, this numerical tool is not robust enough to be able to take in account the whole real problem. The engineer needs to make a good decision on the parameters choice before start analyzing. It is necessary a good calculation planning.

Six sigma methods were introduced in this study to aid the best CAE experiments initial setup. The analysis on this paper was not run in a conventional UNIX workstation, instead the calculation has been performed using Cray super computer. That is because of the need of high resolution on finite elements tooling, where the study surfaces would be represented on detail, especially for the interference between tube and the hub.

Further complete durability analysis, taking in account thickness and different materials, will allow improvement on obtaining a design which satisfies the requirements of material quantity optimization.

Additional iterations analysis in the model was done. It was necessary, because the non linear analysis. The analysis setup was very difficult. The contact modeling was used to determine the best parameters on the model.

If, at least, a good design "starting point" is not known at the earlier phases of the component development, the number of calculus iterations and tests in the conventional design methodologies may increase significantly. And then timing and costs demanded by these conventional methodologies become prohibitive in a competitive market.

7. CONCLUSIONS

On this work is proposed investigation of the best methodology to be applied in the component design (especially press-fit pieces) using CAE, six sigma decision method and experimental data from strain gauges rosettes.

It is common in the automotive industry to use as constructive standard for this type of assembly for press-fit as high values of geometric tolerances to guarantee unfastening of the parts due to the efforts that are submitted. The cost of this joining is the increase of stress concentration factor located on the assembly interface. Therefore it is reasonable to affirm that the value of Kt always will be above of 2. It is also showed that stress concentration factor depends exclusively on the geometry of the parts.

For future works, where Kt is not found on the specific literature, is important to make a correlation between physical test and CAE analysis to define the best way on determining Kt.

On experimental set-ups, for tests and calibration, it is very important to take a great care of the rosettes assembly, especially on the situations where space is restricted. The probability of obtaining unsatisfactory results is very high and closely correlated to the set-up quality.

Further investigation is needed on the field of loading and stress correlation, looking for a better understanding about the relation between local and nominal stress.

8. ACKNOWLEDGEMENT

9. REFERENCES

ABAQUS Simulia Documentation Release 6.7-4;
MINITAB® Release 14.20. Six Sigma Academy Module Release 14.20;
Peterson's Stress Concentration Factors, / Walter D. Pilkey, 1997, 2nd Edition, John Wiley and Sons, Inc ISBN 0-471-53849-3;
Shigley, J.E., C.R. Mischke, Mechanical Engineering Design, 5th Ed., McGraw-Hill, Inc., New York, 1989;
Young, W.C., Roark's Formulas for Stress & Strain, 6th Edition, 1989, ISBN 0-07-100373-8. Determination of stress concentration factors, 2001, Proc, Instn Mech Engrs, Vol 215 Part G;

10. RESPONSIBILITY NOTICE

The authors are the only responsible for the printed material included in this paper.